
Limited Incremental Diagnostic Values of Attenuation-Noncorrected Gating and Ungated Attenuation Correction to Rest/Stress Myocardial Perfusion SPECT in Patients with an Intermediate Likelihood of Coronary Artery Disease

Dong Soo Lee, Young So, Gi Jeong Cheon, Kyeong Min Kim, Myoung Mook Lee, June-Key Chung, and Myung Chul Lee

Departments of Nuclear Medicine and Internal Medicine, Seoul National University College of Medicine, Institute of Radiation Medicine, Seoul National University Medical Research Center, Seoul, Korea

Either gated myocardial perfusion SPECT or attenuation-corrected SPECT can be used to improve specificity in the diagnosis of coronary artery disease (CAD). We investigated whether attenuation-noncorrected gating and ungated attenuation correction could improve the diagnostic performance of rest/stress perfusion SPECT in patients having an intermediate pretest likelihood of CAD. **Methods:** Sixty-eight patients (29 men, 39 women; mean age, 59 ± 12 y) with coronary artery stenosis $\geq 70\%$ (1 vessel, $n = 13$; 2 vessels, $n = 18$; 3 vessels, $n = 8$; normal, $n = 29$) underwent rest attenuation-corrected ^{201}Tl SPECT and dipyridamole stress gated attenuation-corrected $^{99\text{m}}\text{Tc}$ -methoxyisobutyl isonitrile SPECT with an ADAC vertex camera. Three physicians graded the post-test likelihood of CAD for each arterial territory using a 5-point scale (1, normal; 2, possibly normal; 3, equivocal; 4, possibly abnormal; 5, abnormal). The sensitivity, specificity, and areas under receiver-operating-characteristic curves were compared for each operator by 3 methods: attenuation-noncorrected rest/stress SPECT, gated poststress SPECT plus attenuation-noncorrected rest/stress SPECT, and attenuation-corrected rest/stress SPECT plus gated poststress SPECT plus attenuation-noncorrected rest/stress SPECT. **Results:** When higher than grade 3 was used as the criterion for CAD, no differences in sensitivity and specificity were found among the 3 methods for each operator. Areas under receiver-operating-characteristic curves for the diagnosis of CAD and stenosis revealed no differences for each modality ($P > 0.05$ for each comparison). **Conclusion:** In patients with an intermediate risk of CAD, viewing attenuation-noncorrected gated poststress SPECT and ungated attenuation-corrected rest/stress SPECT images did not improve the diagnostic performance for CAD and stenosis.

Key Words: CAD; gated myocardial SPECT; attenuation-corrected SPECT; ROC analysis; $^{99\text{m}}\text{Tc}$ -MIBI

J Nucl Med 2000; 41:852–859

Gated myocardial SPECT has been reported to have additive diagnostic value for differentiating between false-positive and true-negative findings of conventional ungated rest/stress myocardial SPECT (1). Gated wall motion observed on gated rest or poststress SPECT has been used to differentiate between fixed defects and attenuation artifacts of resting images (2). If the myocardial wall appeared to have a fixed defect that moved well, perfusion of this segment permitted contraction to occur, and the apparent fixed defect was not real. Gated myocardial SPECT, by revealing resting wall motion, has shown that this apparent fixed defect was associated with the effect of attenuation (3). Therefore, a true fixed defect that appeared to be borderline abnormal could be easily discriminated from an artifact by reference to gated myocardial SPECT (2,4). However, only resting-state wall motion information was obtained by gated SPECT acquired either at rest or during the poststress period.

Attenuation-corrected myocardial SPECT can compensate for the inhomogeneous attenuation effect of chest wall and tissues around the heart (5). Attenuation correction has been applied to both resting and stress myocardial images and indicated that the apparent resting or stress defect was caused by attenuation. In the diagnosis of coronary artery stenosis and coronary artery disease (CAD), attenuation correction enhanced the specificity or normalcy ratio for the diagnosis of CAD (5,6) and helped in the diagnosis of patients with a low pretest likelihood of disease (7,8). Attenuation correction improved the homogeneity of the myocardial walls in subjects with a low pretest likelihood of disease and ensured that segments that were apparently borderline normal were in fact normal (9). Because radioactivity in healthy subjects was quite homogeneous on attenuation-corrected SPECT, readers were thus able to pick out

Received Dec. 14, 1998; revision accepted Jul. 9, 1999.

For correspondence or reprints contact: Dong Soo Lee, MD, Department of Nuclear Medicine, Seoul National University College of Medicine, 28 Yungun-dong Chongnogu, Seoul 110-744, Korea.

subtle hypoperfused areas so that diagnostic accuracy of multivessel or left main artery disease also improved significantly (10,11). Because of the proximity of the camera heads, lateral wall activity was often overestimated on conventional attenuation-noncorrected SPECT; however, lateral wall hypoperfusion can be discerned more easily after attenuation correction (10–12). Furthermore, the degree of improvement in diagnostic accuracy does not vary according to patients' sex or degree of obesity (13–15).

Because prognostic predictive values of SPECT have been found to differ according to the pretest likelihood (16,17), the diagnostic accuracy of myocardial SPECT is closely related to the pretest likelihood of CAD. Therefore, the selection of a target population to test the diagnostic performance of myocardial SPECT might be based on this criterion. The aim of performing myocardial SPECT differs according to the pretest likelihood. In patients in whom this pretest likelihood is high, myocardial SPECT is performed to determine which arterial territory is ischemic or related to the infarct. In patients with a very low likelihood of CAD (<5%), myocardial SPECT is performed to confirm normal perfusion (1,6–8,18). In this study, we hypothesized that either gating or attenuation correction (or both) improved diagnostic accuracy only when it had been confirmed that adding gated poststress SPECT or attenuation-corrected ungated rest/stress SPECT improved diagnostic accuracy in patients with an intermediate pretest likelihood of CAD.

We investigated using receiver-operating-characteristic (ROC) curve analysis to determine whether diagnostic accuracy was improved by adding gating or attenuation correction in patients with an intermediate pretest likelihood of CAD who were assessed using the methods of Pryor et al. (19). ROC curve analysis (20–22) was used to compare the diagnostic performance of conventional rest/stress myocardial SPECT and the sequential addition of gated poststress attenuation-noncorrected SPECT and attenuation-corrected ungated SPECT with conventional rest/stress SPECT.

MATERIALS AND METHODS

Patients

Among 1393 sequential patients who had myocardial perfusion SPECT between June 1996 and August 1997, we selected 173 patients for subsequent coronary angiography within 2 mo of

myocardial SPECT. On the basis of the method of Pryor et al. (16), a pretest likelihood was calculated, and an intermediate pretest likelihood was defined as 15%–85%. Sixty-eight patients (29 men, 39 women; mean age, 59 ± 12 y) with an intermediate likelihood of CAD were included in this study.

The average pretest likelihood of patients was $60\% \pm 20\%$. A decrease in coronary artery diameter of $\geq 70\%$, as seen on coronary angiography, was considered significant stenosis. Thirty-nine patients had CAD in 1 of the 3 main vessels or their major branches: 13 had single-vessel disease, 18 had 2-vessel disease, and 8 had triple-vessel disease.

Twenty-nine patients had stenosis of the left anterior descending artery, 23 had stenosis of the left circumflex artery, and 21 had stenosis of the right coronary artery. No patients had left main artery disease.

Acquisition of Attenuation-Corrected Rest and Gated Attenuation-Corrected Stress Myocardial SPECT

An attenuation-corrected rest ^{201}Tl SPECT image was acquired first. Then, a gated attenuation-corrected stress $^{99\text{m}}\text{Tc}$ -methoxyisobutyl isonitrile (MIBI) SPECT image was acquired after dipyridamole stress (Fig. 1). Gated attenuation-corrected SPECT yielded 3 sets of images from a single simultaneous transmission–emission study: ungated attenuation-noncorrected SPECT, gated attenuation-noncorrected SPECT, and ungated attenuation-corrected SPECT.

For ungated attenuation-corrected rest ^{201}Tl SPECT, we administered 111 MBq ^{201}Tl and acquired the SPECT image using a vertical camera (Vertex EPIC; ADAC Laboratories, Milpitas, CA) with a low-energy, all-purpose collimator (VXHR; ADAC Laboratories) and Vantage 1.5 acquisition software (ADAC Laboratories). Each detector rotated in a circular orbit of 90° from the left posterior oblique and 90° from the left anterior oblique orientations, respectively. Thirty-two step-and-shoot images were acquired, with 25 s per step and an interval of 3° . A ^{153}Gd source was used for transmission. The energy window was set at 72 keV (20%) for ^{201}Tl and at 100 keV (20%) for ^{153}Gd . For ungated attenuation-corrected rest ^{201}Tl images, acquisition lasted 15 min.

For gated attenuation-corrected stress $^{99\text{m}}\text{Tc}$ -MIBI SPECT, dipyridamole (0.14 mg/kg/min) was administered for 4 min, and 925 MBq $^{99\text{m}}\text{Tc}$ -MIBI was injected 3 min later. Patients had 1 egg and 360 mL milk as a fatty meal. After 30 min or later, $^{99\text{m}}\text{Tc}$ -MIBI SPECT images were acquired. An acquisition protocol with an interval of 3° with 32 steps of 25 s was used. Gating was performed with 16 frames per cardiac cycle and a matrix of 64×64 . ^{153}Gd was used for the transmission source. Energy windows were set at 140 keV (20%) for $^{99\text{m}}\text{Tc}$ and at 100 keV (20%) for ^{153}Gd .

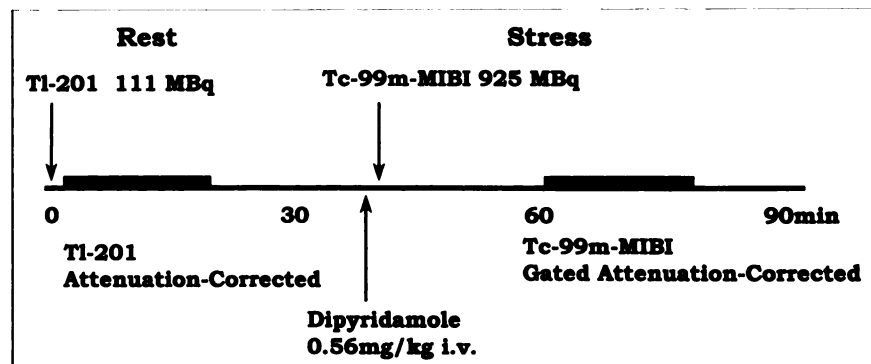


FIGURE 1. Methods of attenuation-corrected rest ^{201}Tl SPECT and dipyridamole stress gated attenuation-corrected $^{99\text{m}}\text{Tc}$ -MIBI SPECT. i.v. = intravenously.

Reconstruction of Attenuation-Noncorrected Ungated Images, Gated Stress Images, and Attenuation-Corrected Ungated Images

Resting ^{201}Tl projection images were split into emission and transmission images. Stress $^{99\text{m}}\text{Tc}$ -MIBI projection images were split automatically into gated emission images, ungated emission images, and transmission files. Split gated and ungated projection files were equivalent to gated and ungated SPECT projection files, respectively, acquired with the transmission sources off.

Attenuation-noncorrected ungated rest ^{201}Tl images were reconstructed using a Butterworth filter with a cutoff frequency of 0.4 and an order of 5. Attenuation-noncorrected ungated stress $^{99\text{m}}\text{Tc}$ -MIBI images were reconstructed using a Butterworth filter with a cutoff frequency of 0.66 and an order of 5. Reconstructed images were reoriented to conventional short-axis, vertical long-axis, and horizontal long-axis images.

With ungated transmission projection files from ^{201}Tl and $^{99\text{m}}\text{Tc}$ -MIBI SPECT images, resting and stress attenuation maps were reconstructed using a Butterworth filter with a cutoff frequency of 0.5 and an order of 5. Using these attenuation maps and reconstructed attenuation-noncorrected ungated rest and stress images, we iteratively reconstructed attenuation-corrected images using a maximum likelihood expectation maximization algorithm. Attenuation-noncorrected ungated rest and stress images were used as primers. Iteration was stopped after 12 iterations according to recommendation of the manufacturer (ADAC Laboratories).

Poststress $^{99\text{m}}\text{Tc}$ -MIBI gated SPECT images were reconstructed using a Butterworth filter with a cutoff frequency of 0.66 and an order of 5. Reconstructed gated images were reoriented to short-axis, vertical, and horizontal long-axis images and displayed in 3 dimensions using Cedars quantitative gated SPECT software (ADAC Laboratories).

Image Interpretation

Three operators who were unaware of the clinical pretest likelihood, final diagnosis, or each other's results read 68 image sets from the patients with an intermediate pretest likelihood of CAD.

Attenuation-noncorrected ungated rest and stress images were interpreted visually. Keeping in mind attenuation-noncorrected ungated rest and stress images, poststress gated images were interpreted; these images were displayed on a 3-dimensional mode using end-diastolic mesh and a moving plane inside this mesh. With both findings in mind, attenuation-corrected ungated rest SPECT images were interpreted visually.

Both reversible and persistent perfusion abnormalities found on attenuation-noncorrected SPECT were considered to indicate significant stenosis of the related coronary artery. If significantly decreased perfusion was found at 1 of 3 artery territories, the patient was considered to have CAD.

The degree of confidence of significant perfusion decrease was scored from grade 1 to grade 5: grade 1, definitely normal; grade 2, probably normal; grade 3, equivocal; grade 4, probably abnormal; and grade 5, definitely abnormal. The highest score among the scores of the 3 territories was used to indicate the score of the patient. To represent the attitudes of the readers in scoring definite grades (1 and 5), the percentages of grades with definiteness (definitely normal and definitely abnormal) were calculated—that is, the (number of grades 1 and 5)/(total number of grades 1 through 5). The 3 physicians had 4, 7, and 11 y of experience in interpreting attenuation-noncorrected ungated resting and stress myocardial

SPECT. They had trained themselves to read poststress gated SPECT images in the clinical setting for 3 y before this study. They had experience interpreting 1200 studies of attenuation-corrected ungated resting and stress myocardial SPECT for 1 y and tried to build norms of their own because the attenuation-corrected normal distribution is different from the attenuation-noncorrected normal distribution.

Statistical Analysis

The areas under curves (AUCs) of attenuation-noncorrected SPECT were calculated and compared with the AUCs of attenuation-noncorrected SPECT and gated SPECT together. Furthermore, the AUCs of attenuation-noncorrected SPECT, gated SPECT, and attenuation-corrected SPECT together were calculated and compared with the AUCs of attenuation-noncorrected SPECT and gated SPECT together.

The AUC was calculated using Hanley and McNeil's method (20). We calculated the probability of choosing the correct combined pair of abnormal and normal images from the pool of 29 normal (x_N) and 39 abnormal (x_A) images. This probability was considered to represent the discriminatory performance of each method. The nonparametric test index W was calculated as:

$$W = \frac{1}{39 \times 29} \sum_{i=1}^{39} \sum_{j=1}^{29} S(x_A, x_N).$$

W has been reported to be equivalent to the AUC (20). The SE of W was calculated using the true AUC and Q_1 and Q_2 , which were indices of the probability of discriminating images correctly among 3 images selected randomly from the whole pool of images (20). After obtaining estimates of the AUC and the SEs, the statistical significance of differences was determined. Differences between the AUCs of attenuation-noncorrected images and of attenuation-noncorrected plus gated images were calculated; then those between the AUCs of attenuation-noncorrected plus gated images and of attenuation-noncorrected plus gated plus attenuation-corrected images were calculated. Using the following equation, SEs were compensated by considering paired characteristics of these data:

$$SE(\text{Area}_1 - \text{Area}_2) = \sqrt{\frac{SE^2(\text{Area}_1) + SE^2(\text{Area}_2) - 2rSE(\text{Area}_1)SE(\text{Area}_2)}{2}}.$$

In this equation, r was calculated by averaging Pearson's correlation coefficients of normal and abnormal images. The z value,

$$\left[z = \frac{\text{Area}_1 - \text{Area}_2}{SE(\text{Area}_1 - \text{Area}_2)} \right],$$

was assumed to have a normal distribution. We tested the null hypothesis that z would be zero and compared the AUCs of the 3 methods. To compensate for the effect of multiple comparisons, the Bonferroni correction was adopted. For practical calculation, MedCalc Software (MedCalc Software, Mariakerke, Belgium) was used.

RESULTS

Diagnostic Accuracy

Table 1 shows grades of segmental perfusion decrease for each artery territory scored by operator 1 after assessing all 3 images: attenuation-noncorrected rest/stress, gated post-stress, and attenuation-corrected rest/stress. Among 204

TABLE 1
Perfusion Decrease Findings of Operator 1
Using Conventional Plus Gated Plus
Attenuation-Corrected SPECT

Perfusion decrease	LAD	LCX	RCA	Sum
Reversible	20	4	10	34
Partially reversible	4	3	5	12
Persistent			3	3
Rest decrease more severe than stress decrease	1		1	2
Normal	43	61	49	153
Sum	68	68	68	204

LAD = left anterior descending artery; LCX = left circumflex artery; RCA = right coronary artery.

arterial territories, 153 were normal, 34 showed a reversible perfusion decrease, 12 showed a partially reversible perfusion decrease, 3 showed a persistent decrease, and 2 showed a rest decrease more severe than the stress decrease. When higher than grade 3, the perfusion decrease was taken to indicate CAD. The sensitivity and specificity for operator 1 were 67% and 76%, respectively, using attenuation-noncorrected rest/stress SPECT. For operator 2, sensitivity and specificity were 67% and 83%, respectively, and for operator 3, they were 71% and 51%, respectively.

ROC Curve Analysis for Diagnosis of CAD

Figure 2 shows ROC curves for attenuation-noncorrected SPECT, attenuation-noncorrected plus gated SPECT, and attenuation-noncorrected plus gated plus attenuation-corrected SPECT. The AUCs of 3 ROC curves for operator 1 were 0.765, 0.717, and 0.768 (Table 2); there was no stepwise statistical difference. The AUCs for operator 2 were 0.790, 0.776, and 0.798; again, these results were not significantly different between methods. The AUCs for operator 3 were 0.712, 0.685, and 0.781, and there was a significant difference between the AUC of attenuation-noncorrected plus gated SPECT and attenuation-noncor-

TABLE 2
AUCs of ROC Curves of Attenuation-Noncorrected SPECT
Plus Gated SPECT Plus Attenuation-Corrected SPECT

Method	Operator 1	Operator 2	Operator 3
Attenuation-noncor- rected SPECT	0.765	0.790	0.712
Plus gated SPECT	0.717	0.776	0.685
Plus attenuation- corrected SPECT	0.768	0.798	0.781

rected plus gated plus attenuation-corrected SPECT ($P = 0.02$). However, no difference was found between attenuation-noncorrected and attenuation-corrected SPECT ($P = 0.15$).

ROC Curve Analysis for Diagnosis of Significance of Individual Coronary Artery Stenosis

Table 3 shows the AUCs of ROC curves for detecting stenosis of CAD using attenuation-noncorrected SPECT, attenuation-noncorrected plus gated SPECT, and attenuation-noncorrected plus gated plus attenuation-corrected SPECT. The AUC for the left anterior descending artery was 0.641–0.734; for the left circumflex artery, it was 0.571–0.765; and for the right coronary artery, it was 0.687–0.819. The AUCs were not significantly different between the 3 methods.

Comparison of Sensitivity and Specificity Between 3 Methods

When higher than grade 3 was regarded as significant, the sensitivity and specificity for operator 1 were 67% and 76%, respectively, with attenuation-noncorrected SPECT. The sensitivity and specificity were 67% and 72%, respectively, with gated SPECT; and they were 69% and 79%, respectively, with attenuation-corrected SPECT. No significant difference was found between the sensitivity and specificity of the 3 methods. For operator 2, the sensitivities of each method were 67%, 69%, and 74%, respectively, whereas the

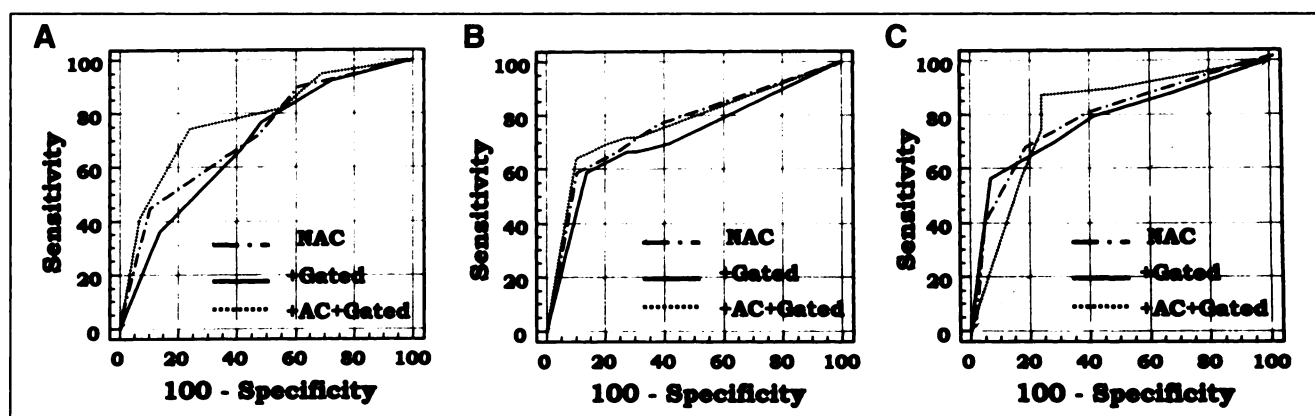


FIGURE 2. ROC curves for diagnosis of CAD for operators 1 (A), 2 (B), and 3 (C). Each step is attenuation-noncorrected (NAC) rest/stress SPECT (before attenuation correction), conventional plus gated SPECT (+Gated), and attenuation-corrected (AC) rest/stress SPECT (+AC+Gated).

TABLE 3
AUCs of ROC Curves for Diagnosis of CAD*

Method	Operator 1	Operator 2	Operator 3
Left anterior descending artery			
Attenuation-noncorrected SPECT	0.686	0.693	0.641
Plus gated SPECT	0.681	0.694	0.668
Plus attenuation-corrected SPECT	0.734	0.717	0.680
Left circumflex artery			
Attenuation-noncorrected SPECT	0.571	0.618	0.616
Plus gated SPECT	0.571	0.765	0.607
Plus attenuation-corrected SPECT	0.617	0.765	0.612
Right coronary artery			
Attenuation-noncorrected SPECT	0.759	0.782	0.687
Plus gated SPECT	0.751	0.846	0.725
Plus attenuation-corrected SPECT	0.785	0.819	0.770

*Areas are not significantly different.

specificities were 83%, 72%, and 76%, respectively. No significant difference was found between methods. The sensitivities for operator 3 were 71%, 67%, and 74%, respectively, and the specificities were 51%, 58%, and 75%, respectively. Again, no difference was found between methods.

For each arterial territory, the diagnostic sensitivity and specificity between the 3 methods—namely, attenuation-noncorrected SPECT, attenuation-noncorrected plus gated poststress SPECT, and attenuation-noncorrected plus gated poststress plus attenuation-corrected SPECT—were not significantly different.

Grade Changes of Each Operator When Viewing Further Gated SPECT and Attenuation-Corrected SPECT Images

For operator 1, the ratios of grades 1 and 5 (definite grades) to the total number of grades were 78% with attenuation-noncorrected SPECT, 82% with attenuation-noncorrected plus gated SPECT, and 85% with attenuation-noncorrected plus gated plus attenuation-corrected SPECT (Fig. 3A). The ratios of definitive grades increased but not to statistically significant levels because for attenuation-noncorrected SPECT, the ratio of definitive grades was already high (79% for the left anterior descending artery, 94% for the left circumflex artery, and 87% for the right coronary artery). Even though the ratios of definitive grades increased stepwise in the diagnosis of each arterial stenosis, their effects were minimal.

For operator 2, the ratio of definitive grades increased from 29% with attenuation-noncorrected SPECT to 57% with attenuation-noncorrected plus gated SPECT to 68% of attenuation-noncorrected plus gated plus attenuation-corrected SPECT (Fig. 3B). However, for each artery, the

ratio per step did not increase. The final definite grades were 65% for the left anterior descending artery, 81% for the left circumflex artery, and 72% for the right coronary artery.

For operator 3, the ratio of definite grades did not change after viewing gated or attenuation-corrected SPECT images (Fig. 3C). The ratios of definite grades were 40%, 43%, and 43% for the 3 methods. Again, the ratio per step did not increase. The final definite grades were 53% for the left anterior descending artery, 72% for the left circumflex artery, and 58% for the right coronary artery.

DISCUSSION

By displaying resting wall motion, gated SPECT helped differentiate true fixed perfusion defects from artifacts. If resting wall motions were normal, then perfusion in that segment was normal and the apparent perfusion decrease at rest was an artifact (2). If decreased uptake during stress was similar to that seen during the resting period and that segment showed good wall motion, the apparent hypoperfusion during stress was also an artifact. However, when decreased uptake was found only during a period of stress, or when it was necessary to differentiate a reversible decrease from an artifact, gated SPECT was no longer helpful.

Artifacts are associated primarily with attenuation (23). Experienced physicians can discriminate attenuation artifacts using projection files and planar images and by comparing stress and rest differences (23).

Smanio et al. (1) recently suggested that gated SPECT could improve diagnostic accuracy in 2 ways. In subjects with a low pretest likelihood of CAD (<10%; n = 137), the normal rate increased significantly if gated SPECT images were evaluated; in patients with both CAD and myocardial infarction (n = 49), the true-positive ratio also increased.

To assess whether additional information acquired from gating or attenuation correction is helpful, the number of false-positive segments must be known before gated or attenuation-corrected SPECT images are interpreted (3). In this study, we found only 3 false-positive cases among 51 significantly stenosed arteries and thus found no additional advantage in either method. Similar issues were raised by Kang et al. (24), who found that, in routine reading, the frequency of persistent defect was so low that gated SPECT was thus not very helpful. The lower prevalence of persistent defect could be attributed to population difference or characteristics of the population with an intermediate pretest likelihood (or both) in our study. The pretest likelihood of CAD or a history of myocardial infarction was probably related with the prevalence of persistent defects.

In an early report by DePuey and Rozanski (2) referring to the diagnostic usefulness of gated SPECT, the efficacy of gated SPECT relied on a history of myocardial infarction. In 102 patients with such a history, these authors determined that all fixed defects were real. On the other hand, they determined the 60 of 78 patients with no history of myocardial infarction by observing normal wall motion. If

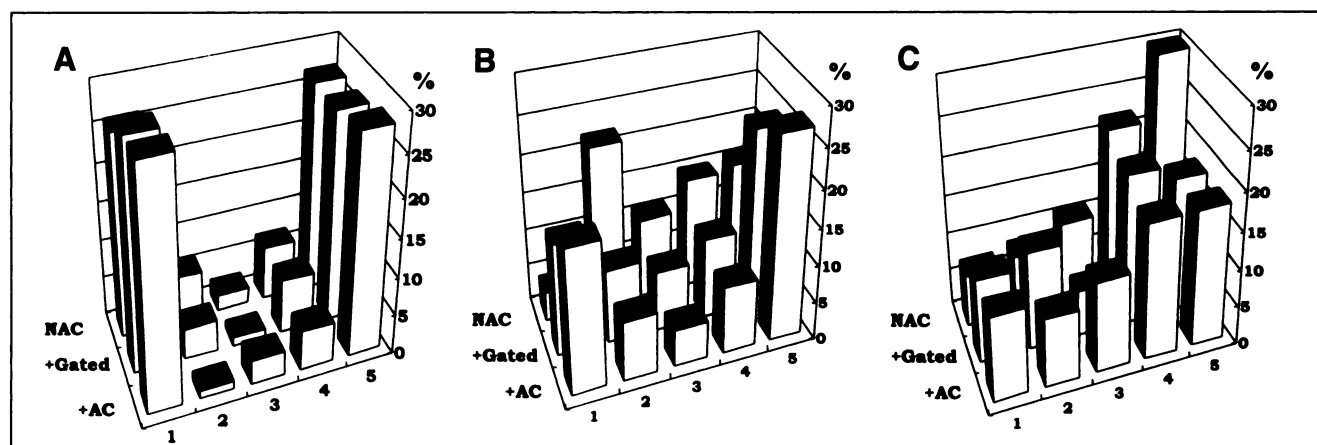


FIGURE 3. Changes in scoring characteristics for operators 1 (A), 2 (B), and 3 (C). Each step is same as in Figure 2. Grade 1 means definitely normal; grade 2, probably normal; grade 3, equivocal; grade 4, probably abnormal; and grade 5, definitely abnormal. Height of bar indicates percentage of each grading/total number of grading. NAC = nonattenuation-corrected; AC = attenuation-corrected.

these 78 patients were considered normal because they had no history of myocardial infarction and had a low pretest likelihood (<5%) before the SPECT study, we doubt that DePuey and Rozanski would have had difficulty in proving the efficacy of gated SPECT in defining normal.

Experienced operators finalize their reading by considering the patient's history and the pretest likelihood when comparing stress and rest images. If informed that the pretest likelihood of these patients is low, they tend to decide that an apparent defect is an artifact; if the pretest likelihood is high, they classify the defect as real. In this group of patients, using conventional rest/stress SPECT, we try to determine which arterial territory is responsible for stress-induced ischemia. When evaluating the efficacy of a diagnostic test, the pretest likelihood is thus important.

In this study, factors such as age, sex, smoking history, lipid serum concentration, types of chest pain, history of infarction, rest electrocardiogram, and history of diabetes were used to assess the pretest likelihood of CAD according to the report of Pryor et al. (19). We considered a probability of 15%–85% as an intermediate likelihood. We hypothesized that these new methods would be very helpful if we could prove the diagnostic efficacy of gated or attenuation-corrected SPECT in patients with an intermediate pretest likelihood.

In patients with a pretest likelihood of less than 5% or 10%, myocardial circumferential profiles became more homogeneous by attenuation correction (6,9). Several reports have stated that the normalcy ratio, used to identify low-likelihood subjects, improved significantly after evaluating attenuation-corrected SPECT (5–8). These investigators reached consensus in this regard and, furthermore, maintained that sensitivity had improved. We suspect, however, that because physicians were relieved about the homogeneity of normal walls, they were able to determine decreased myocardial uptake more definitively and confidently. Preliminary reports have shown that, in triple-vessel or left main disease, attenuation correction helped to detect a “balanced”

decrease of myocardial uptake or mild decrease in wider areas of the myocardium. Because overestimation of uptake was moderated by attenuation correction, they were more easily able to determine lateral wall abnormality (10–12).

We did not include left main artery disease in our group of patients, and there were 8 patients with triple-vessel disease among the total 68. These 8 patients were not treated separately. Twenty-three patients had left circumflex disease, but attenuation correction did not significantly increase diagnostic accuracy. We initially hypothesized that gating or attenuation correction would help differentiate an inferior wall, but we found no evidence that these methods increased diagnostic performance in that region in this patient population of intermediate likelihood.

Gated SPECT grades for operator 2 tended toward both ends of the scale (definitely normal or abnormal) after viewing attenuation-corrected images—that is to say, this operator's grades became more definite. In contrast, operator 1 tended to score grade 1 or grade 5 in conventional attenuation-noncorrected SPECT and changed grades only slightly after viewing gated or attenuation-corrected SPECT images. Similarly, operator 3 changed his grades slightly after viewing gated or attenuation-corrected SPECT images.

These 3 operators read in different ways, but using the 3 methods, the differences in their conclusions were no greater in a statistical sense than those observed after repeated readings of the same SPECT images. Because we found no increments in the AUC with gated or attenuation-corrected SPECT, we concluded that in patients whose pretest likelihood of CAD was intermediate, stepwise addition of gated poststress SPECT and attenuation-corrected rest/stress SPECT did not add incremental diagnostic value.

The sensitivity or specificity obtained by the 3 different methods was averaged and found not to differ significantly between the 3 operators (Fig. 4). The sensitivity was slightly higher and the specificity was slightly lower for operator 3 than for the others.

The AUC was calculated using Hanley and McNeil's

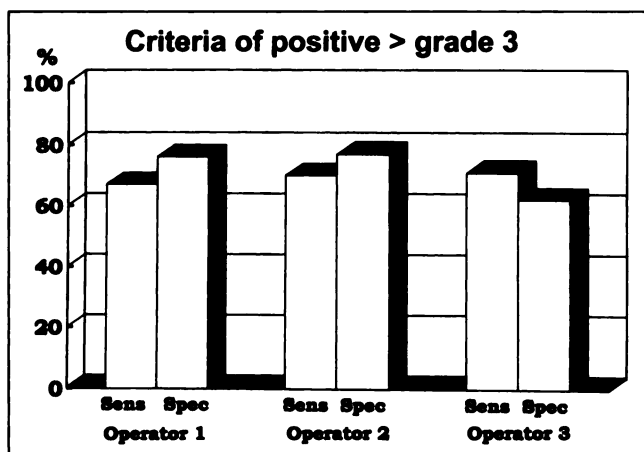


FIGURE 4. Average diagnostic accuracy of each operator. Sens = sensitivity; Spec = specificity.

method (20). We used their Wilcoxon statistics and so tended to obtain a slightly smaller area (conservative estimate) than with the Gaussian fitting of curves and consequent area calculation. A type II error representing the power of statistical testing is one whose significant difference could be missed and therefore in this study deserved our due attention. We tried to decrease the possibility of underestimation of this statistical power by calculating the AUC taking into consideration paired characteristics of our data according to Hanley and McNeil's method (21). Because we had hypothesized that there was incremental value, it was, in a strict sense, necessary to perform a 1-tailed comparison test. Each operator made each comparison twice; however, the Bonferroni correction should have been applied. Taking both facts into consideration, P was set at <0.05 . Statistical sequential repetitive testing was performed for the 3 operators so the statistical difference could have been overestimated. However, this type of error was not compensated for because this effect of overestimation would have increased the type I error but we did not find any significant difference.

The largest difference between the AUCs, which were 0.691 and 0.765, was 0.147. According to the table presented by Hanley and McNeil (20), several hundred subjects should have been recruited to prove that this difference was significant. We studied only 68 patients; accordingly, increasing this sample size 5 times or more might have enabled us to observe differences between the methods. Therefore, from the statistical point of view, a final conclusion should be deferred.

The performance of operator 3 increased stepwise from 0.687 to 0.725 to 0.770. This operator had the least experience among the operators, and we therefore thought it likely that operator experience would relate to the incremental diagnostic performance of gated or attenuation-corrected SPECT. Further studies are required to determine the incremental efficacy of gated and attenuation-corrected SPECT observed in less-experienced physicians (25).

Over a period of 1 y we interpreted >1000 attenuation-corrected ungated resting ^{201}Tl and stress $^{99\text{m}}\text{Tc}$ -MIBI SPECT

images. When we read attenuation-corrected images, we applied different normal distributions of wall uptake according to our experience. However, we could not be certain that we used the best standards for interpreting attenuation-corrected SPECT. We did not use a quantitative approach in this study, and we admit that a quantitative approach could have enhanced the diagnostic capability of attenuation-corrected SPECT better than that of attenuation-noncorrected SPECT. The generation and switching of normal files and the application of a quantification program such as Cequal are now warranted to prove this advantage of attenuation correction. Furthermore, scatter and attenuation correction would have additive value but was not attempted. This study evaluated 1 of the commercially available methods of attenuation correction.

Most previous investigators observed that gating was helpful in differentiating real fixed defects from artifacts; however, gating was not helpful in finding arteries that are significantly stenotic and usually have a reversible decrease in patients with an intermediate pretest likelihood. Gating would have proven to have an incremental value for the diagnosis of coronary artery stenosis in patients with a history of infarction (2). This study does not preclude the possible value of gating to diagnose viable, stunned, or hibernating myocardium. This study did not include a comprehensive assessment of the promising diagnostic role of gating for evaluation of function and perfusion at the same time.

If we select a subgroup with an intermediate likelihood of CAD, such groups need the support of newer technology most because more equivocal cases exist; we clearly showed by ROC curve analysis that, for such groups, addition of attenuation correction did not help in the diagnosis of coronary artery stenosis. This finding explains why the present system of attenuation correction is not commonly adopted or referred to by many laboratories. The cost of the transmission source of the present system was not justified according to this study's results. The present attenuation-correction system is developed insufficiently and the methodological improvement of scatter or resolution correction (or both) is warranted.

CONCLUSION

In myocardial SPECT, determination of the incremental diagnostic efficacy of newer supplementary technology depends crucially on the number of false-positive findings determined to be present with conventional attenuation-noncorrected SPECT. When attention was focused on patients in whom the pretest likelihood of CAD was of intermediate degree, the incremental value of gated or attenuation-corrected SPECT was not found to differ significantly from the value of conventional SPECT.

REFERENCES

1. Smanio PE, Watson DD, Segalla DL, Vinson EL, Smith WH, Beller GA. Value of gating of technetium-99m-sestamibi single-photon emission computed tomographic imaging. *J Am Coll Cardiol*. 1997;30:1687-1692.

2. DePuey GE, Rozanski A. Using gated technetium-99m-sestamibi SPECT to characterize fixed myocardial defects as infarct or artifact. *J Nucl Med.* 1995;36:952-955.
3. Lee DS. New imaging techniques in myocardial perfusion SPECT. *Korean J Nucl Med.* 1998;32:1-9.
4. Miles KA. How does gated SPET alter reporting of myocardial perfusion studies? *Nucl Med Commun.* 1997;18:915-921.
5. Ficaro EP, Fessler JA, Shreve PD, Kirtzman JN, Rose PA, Corbett JR. Simultaneous transmission/emission myocardial perfusion tomography: diagnostic accuracy of attenuation-corrected ^{99m}Tc-sestamibi single-photon emission computed tomography. *Circulation.* 1996;93:463-473.
6. Prvulovich EM, Lonn AHR, Bomanji JB, Jarritt PH, Ell PJ. Effect of attenuation correction on myocardial thallium-201 distribution in patients with a low likelihood of coronary artery disease. *Eur J Nucl Med.* 1997;24:266-275.
7. Fanti S, Dondi M, Guidalotti PL, Fagoli G, Corbelli C, Monetti N. Transmission-emission attenuation correction of myocardial SPECT: impact of false positive rate in a population at low risk of CAD [abstract]. *J Nucl Med.* 1997;38:84P.
8. Hendel RC, Follansbee WP, Heller GV, Cullom SJ, Berman DS. Comparison of exercise and vasodilator stress myocardial perfusion SPECT imaging for the determination of normalcy rate and the effects of attenuation correction [abstract]. *J Am Coll Cardiol.* 1997;29:302A.
9. Kluge R, Sattler B, Seese A, Knapp WH. Attenuation correction by simultaneous emission-transmission myocardial single-photon emission tomography using a technetium-99m-labelled radiotracer: impact on diagnostic accuracy. *Eur J Nucl Med.* 1997;24:1107-1114.
10. Duvernoy CS, Ficaro EP, Karavajakian PA, Rose PA, Corbett JR. Left main coronary disease: increased sensitivity with quantitative attenuation corrected SPECT perfusion imaging [abstract]. *J Am Coll Cardiol.* 1997;29:302A.
11. Ficaro EP, Duvernoy CS, Karavajakian PA, Corbett JR. Evaluation of attenuation corrected cardiac SPECT perfusion imaging in patients with multi-vessel disease [abstract]. *Circulation.* 1997;96:1-308.
12. Barbarisi MJ, Araujo LI, McCellan JR, Alavi A. Attenuation correction improves the assessment of lateral wall perfusion defects on SPECT imaging [abstract]. *J Nucl Med.* 1997;38:84P.
13. Prvulovich EM, Lonn AH, Bomanji JB, Jarritt PH, Ell PJ. Transmission scanning for attenuation correction of myocardial ²⁰¹Tl images in obese patients. *Nucl Med Commun.* 1997;18:207-218.
14. He Z-X, Lakkis NM, America Y, et al. Qualitative and quantitative comparison of sestamibi SPECT without and with attenuation correction for detection of coronary artery disease in patients with large body habitus [abstract]. *J Am Coll Cardiol.* 1997;29:302A.
15. McCellan JR, Viggiano J, Alavi A, Araujo LI. Lack of gender differences in Tc-99m sestamibi tomographic myocardial perfusion images obtained with attenuation correction and enhanced acquisition methods [abstract]. *J Am Coll Cardiol.* 1997;29:303A.
16. Berman DS, Hachamovich R, Kiat H, et al. Incremental value of prognostic testing in patients with known or suspected ischemic heart disease: a basis for optimal utilization of exercise technetium-99m sestamibi myocardial perfusion single-photon emission computed tomography. *J Am Coll Cardiol.* 1995;26:639-647.
17. Corbett JR, Karabajakian MZ, Rose PA, Ficaro EP. The effect of attenuation correction on cardiac risk assessment using dual isotope myocardial perfusion imaging with rest Tl-201 and stress Tc-99m-sestamibi [abstract]. *J Nucl Med.* 1997;38:83P.
18. Holly TA, Parker MA, Leonard SM, Toth BM, Hendel RC. Comparative diagnostic accuracy of gated SPECT and attenuation in myocardial perfusion imaging [abstract]. *Circulation.* 1997;96:1-442.
19. Pryor DB, Harrel FE Jr, Lee KL, Califf RM, Rosati RA. Estimating the likelihood of significant coronary artery disease. *Am J Med.* 1983;75:771-780.
20. Hanley JA, McNeil BJ. The meaning and use of the area under a receiver operating characteristic (ROC) curve. *Radiology.* 1982;143:29-36.
21. Hanley JA, McNeil BJ. A method of comparing the areas under receiver operating characteristic curves derived from the same set of cases. *Radiology.* 1983;148:839-843.
22. DeLong ER, DeLong DM, Clarke-Pearson DL. Comparing the areas under two or more correlated receiver operating characteristic curves: a nonparametric approach. *Biometrics.* 1988;44:837-845.
23. DePuey EG, Garcia EV. Optimal specificity of thallium-201 SPECT through recognition of image artifacts. *J Nucl Med.* 1989;30:441-449.
24. Kang WJ, Lee DS, Lee MM, Chung J-K, Lee MC, Koh C-S. Performance of gated myocardial perfusion SPECT to diagnose coronary artery disease. *Korean J Nucl Med.* 1997;31:50-56.
25. Chow T, Chuang ML, Beaudin RA, Riley MF, Douglas PS. Three-dimensional echocardiography improves accuracy and reproducibility of LV ejection fraction estimates by an inexperienced reader [abstract]. *J Am Coll Cardiol.* 1997;29:521A.